Rare Metal Materials and Engineering
Volume 51, Issue 2, February 2022
Available online at www.rmme.ac.cn

Science Press

Cite this article as: Edwin Eyram Klu, Jiang Jinghua, Bassiouny Saleh, et al. Influence of Equal Channel Angular Pressing on Mechanical Properties of Mg-Li Alloys: An Overview[J]. Rare Metal Materials and Engineering, 2022, 51(02): 491-510.

ARTICLE

Influence of Equal Channel Angular Pressing on Mechanical Properties of Mg-Li Alloys: An Overview

Edwin Eyram Klu[1], Jiang Jinghua[1,2], Bassiouny Saleh[1,3], Ma Aibin[1,2], Salifu Nasiru[1], Song Dan[1,2]

[1] College of Mechanics and Materials, Hohai University, Nanjing 210098, China; [2] Suqian Research Institute, Hohai University, Suqian 223800, China; [3] Production Engineering Department, Alexandria University, Alexandria 21544, Egypt

Abstract: Equal channel angular pressing (ECAP) is an effective and efficient severe plastic deformation (SPD) technique used to produce ultrafine grained (UFG) materials with improved properties. This review highlights a comprehensive summary of the mechanical property of various Mg-Li alloys subjected to ECAP processing, the effect of the processing parameters as well as the mechanism involved. This research can also provide directions and supports for the mechanical property improvement of Mg-Li alloys in the future.

Key words: Mg-Li alloys; ECAP; SPD; mechanical property; microstructure

Magnesium (Mg) exists in the earth crust in abundant amounts and percentages[1]. It constitutes about 2% of the earth ' s crust and also constitutes a substantial amount of concentrate in dissolved seawater. As a result, a good amount of magnesium and its compounds are obtained from seawater and lake environments[2]. Magnesium is non-toxic, biocompatible, degrading naturally in the human body and has a comparatively low melting point[3]. Magnesium has a density of 1.7 g/cm^3, which makes it the lightest of all the structural metals. The density of magnesium alloy is approximately far below that of aluminium and steel and is comparable to that of plastics and carbon fiber composites. Magnesium alloys are therefore used where lightweight is of important consideration (aerospace and automobile industries and energy applications) [4-6]. Magnesium is considered to have a hexagonal closed packed (hcp) crystal structure with the major slip system being the basal plane (0001) resulting in its poor room temperature formability[7,8]. The progress in the research of magnesium alloys is geared towards obtaining materials with high strength at room and high temperatures, improved ductility and affordability[9,10]. Magnesium alloys have a vast array of applications[11-13], typically classified as cast and wrought, with the cast alloys being predominant[14,15]. Light material in the automotive and aerospace industry is of high demand, owing to the necessities for environmental safety, reduction in CO_2 emissions and fuel consumption[16-20]. Magnesium based alloys are also used in other numerous applications, including bicycle frames, screen housing, mobile handsets, amongst others[21]. Some biomaterials made from magnesium are also used in orthopedic and cardiovascular fields[22]. In addition, magnesium has a very high chemical activity and high specific energy making it attractive in the manufacture of batteries and its components. Also, the electronegativity of magnesium allows it to be used for sacrificial cathodic protection applications and in the manufacture of dry-cells and cell batteries[23]. However, the high reactivity affinity of magnesium and its alloys in corrosion environments, especially in Cl^- solutions, restricts its application in some engineering and medical fields[24,25]. In medical applications, the rapid deterioration/degradation of magnesium and their alloys can lead to implant failure[26,27]. The chemical composition of magnesium alloys affects their corrosion resistance, behaviour and rate. The surface treatment and finishing also affect their overall corrosion

Received date: February 21, 2021
Foundation item: National Natural Science Foundation of China (51878246, 51979099); Natural Science Foundation of Jiangsu Province of China (BK20191303); Fundamental Research Funds for the Central Universities of Hohai University (B200202122 & 2019B768814)
Corresponding author: Song Dan , Ph. D., Professor, College of Mechanics and Materials, Hohai University, Nanjing 210098, P. R. China, Tel: 0086-25-83786046, E-mail: songdancharls@hhu.edu.cn

behaviour in service[28-30].

Magnesium has extensive use in the nuclear industry, metal, and military aircraft. In the automobile industry, magnesium also has tremendous use with the VW (Volkswagen) Beetle[11,31]. Magnesium alloys have widespread use in the automobile and aerospace industry owing mainly to their relatively low density (strength to weight ratio) as compared to other structural metals and better strength compared to polymers[32,33]. Back in those days, some aircrafts like the B-36 "Peacemaker" were manufactured with incorporations of magnesium alloys[34]. In 1928, Porsche groups assembled their first engine made with magnesium metal[35]. Sir Humphry Davy is historically recognized to have produced pure magnesium metal in 1808 by the reduction of magnesium oxide with potassium vapour. However, the very first industrial production of magnesium took place in 1863 under the supervision of Deville and Caron in France and involved the reduction of a mixture of anhydrous magnesium chloride and calcium fluoride by sodium[36]. The history of Mg and Mg metal production is shown in Fig.1.

Magnesium alloys, despite their super lightweight and high specific strength, still have some deficiencies that need to be resolved, such as relatively low strength, unstable mechanical properties, relatively high production cost[12,32,37]. These drawbacks have necessitated the use of alloying elements to improve such properties. The addition of alloying elements (alloying) is generally effective in obtaining Mg-base alloys with good properties[38]. Different alloying elements present different effects on the overall performance of the alloy[39]. Combinations of different alloys also result in different properties in the overall alloy produced. Therefore, alloying elements are an essential part in determining the mechanical property and corrosion behaviour of the alloy under consideration. Furthermore, the alloying element concentration also plays a major role in its alloying effect[40-42]. Table 1 presents different alloying elements with various effects that they play when found in the alloy structure of a metal. One of the popular and widely used Mg alloys is magnesium-lithium (Mg-Li) alloys[43-45]. Mg-Li alloys are attracting tremendous attention in both the scientific society as well as industrial applications owing to their excellent properties such as super lightweight, relatively high specific strength and stiffness, and good formability[12,46]. However, just like Mg alloys in general, Mg-Li alloys still have drawbacks of low strength, unpredictable mechanical properties as well as poor corrosion resistance[47-50]. Mg-Li alloys with 5.5wt% and 10.2wt% Li exhibit a duplex phase structure consisting of the α-Mg (hcp) and β-Li (bcc) phases at room temperature as depicted in Fig.2[51,52]. The α phase has moderate strength and low formability while the β phase has a relatively better ductility[53,54]. The single β phase structure exists when Li content is higher than 10.2wt%[55-57]. Mg-Li alloys have seen an outburst of acceptance in studies today, and most researchers focus on their lightweight to meet the ever-growing needs of society.

One major research area of magnesium alloys is improving the mechanical properties by severe plastic deformation (SPD) techniques due to their relatively low strength compared to other metals and alloys. Therefore, this review highlights the effect of the process parameters of ECAP, a premiere SPD process technique, on the mechanical properties of Mg-Li alloys.

1 Types of ECAP Processes

ECAP is classified as one of the most significant severe plastic deformation process techniques. SPD is a processing technique that is useful in producing ultrafine-grained (UFG) materials with excellent and enhanced properties, applicable to both metallic and non-metallic materials[58-60]. Severe plastic deformation dates back to the 1950s to the works of Bridgman, who produced a novel scientific work at the time through the combination of high hydrostatic pressure and shear forming, establishing himself at the core of SPD studies till date[59-61]. Research suggests that the strength of Mg-Li alloys can be extensively improved by plastic deformation and alloying[62,63]. It is also well understood from research that

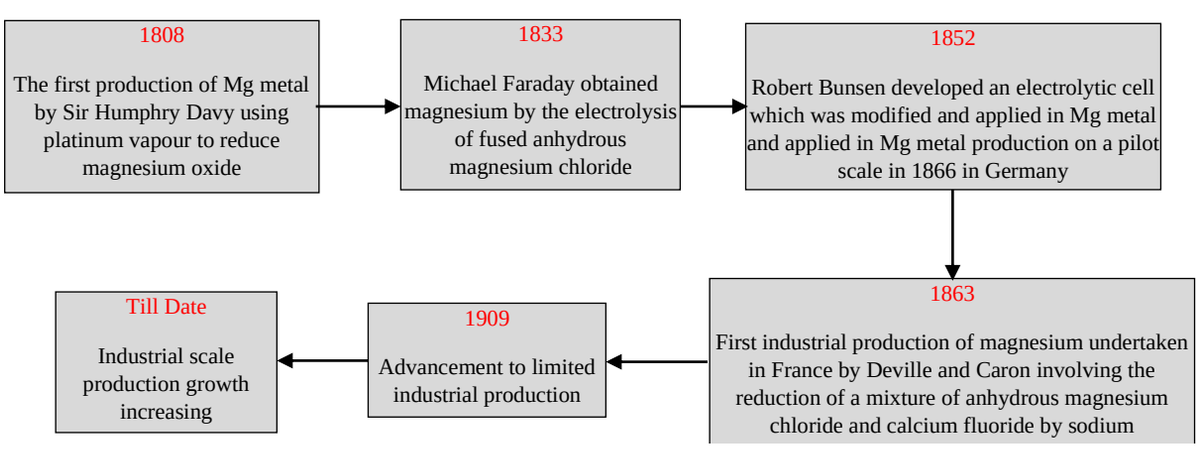

Fig.1 History of Mg and Mg metal production

Table 1 Alloying elements and their effect on Mg-alloy systems[43-45]

Element	Alloying effect
Li	Improving ductility
Ag	Improving high temperature properties and creep resistance when presenting with rare earths
Al	Improving castability, producing precipitation hardening phase, corrosion protection
Ca	Refining grains, improving creep resistance, improving high temperature properties
Be	Improving high temperature properties
Cd	Improving high temperature properties
Ti	Improving high temperature properties, and oxidation resistance
Rare earths	Improving creep resistance, and castability, refining grains, age hardening
Si	Improving creep resistance
Sr	Improving creep resistance
Mn	Improving anti-corrosion behaviour
Y	Improving tensile properties, refining grains
Zn	Improving alloy strength
Zr	Refining grains

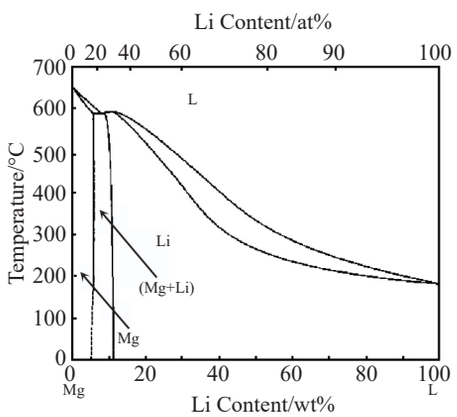

Fig.2 Mg-Li phase diagram[51,52]

conventional deformation processes turn to decrease the ductility of materials which is unacceptable for structural applications, leading to the growing interest in exploring SPD processing techniques that produce UFG materials with excellent mechanical properties[58,64]. Coarse grain, including large secondary phases, have also been studied and shown to result in lower strength[65,66]. Hence, grain size control (especially grain size reduction) has been a key and important requirement for producing materials with excellent properties[59,60] with the formation of finer grains in alloys as compared to pure metals[67,68].

During the SPD process, there is an accumulation of dislocations, and these dislocations interact and tangle with each other, forming low energy configurations leading to the formation of several substructures which share active slip systems[67,69-71]. The rotation of these active slip systems during SPD processes is a key factor in the enhancement of the refinement process[72,73]. Even with intermetallics, there is a string of excellent effects on their ductility, toughness and yield strength when the grain size is reduced appreciably[74,75]. Research also suggests that SPD processes refine grains (which is very vital for superplastic metals) and induce grain growth in the metal structure[76]. This, however, depends on the grain size at the inception of the SPD process as well as the deformation conditions[69,77]. Twinning, when formed during deformation processes usually as coherent twin boundaries, can also disrupt the movement of dislocations and have also been acknowledged as a positive factor to the grain refinement of metals[69,78]. Continuous SPD processing techniques that maximize efficiency are the most popular today. Equal channel angular pressing (ECAP) or equal channel angular extrusion (ECAE) is one of the premiere SPD processes employed by researchers[58,60]. The process as a severe plastic deformation technique dates back to the 1980s to the work conducted by Segal and his team[79,80]. However, its applicability came to light in the 1900s when Valiev and his team developed and applied the process on the production of UFG nanostructures[58,59]. The process is efficient in deforming samples repeatedly without varying their cross-sectional area[79]. There are several types of ECAP processes that have been developed to improve the deformation process and to achieve excellent material property.

1.1 Conventional ECAP

In the conventional ECAP processing technique, a sample either with a square or round cross section is pressed with a plunger through an intersecting die channel with relatively equal cross-sectional areas allowing for repetitive pressing of the sample and retention of initial sample cross section[61,81]. The strain introduced by the ECAP process is generally given by the equation[82, 83]

$$\varepsilon = \frac{N}{\sqrt{3}}\left[2\cot\left(\frac{\phi}{2}+\frac{\psi}{2}\right)+\psi\cos\mathrm{ec}+\left(\frac{\phi}{2}+\frac{\psi}{2}\right)\right] \quad (1)$$

where N is the number of passes, ϕ is the angle of the two intersecting channels and ψ is the opposing angle to the angle made by the intersecting channel. To successfully perform a

large number of passes and to increase the induced strain, the sample billet has to be removed from the die and reinserted for the next pass, making the whole process cumbersome for performing large numbers of passes[84]. During insertion and reinsertion of the billets for pressing, there are several routes and directions, as depicted in Fig.3b. Reinsertion of the billet without any change in direction or rotation is referred to route A. If there is a 90° rotation in the same direction, it is referred to route B_C whiles a 90° rotation in the opposite direction is route B_A. Finally, if the billet is rotated by 180°, it is referred to as route C[85,86]. The conventional ECAP is able to process bulk samples but with limitations in commercial applications[58,86-88]. It also has advantages of being simple and easy to operate as well as improving the strength while keeping a satisfactory ductility compared to the traditional processing methods of rolling, extrusion and drawing which typically improve the strength without increase in ductility[89,90]. Conventional ECAP is generally good at introducing high strain rate ~10^{-1} s^{-1} superplasticity in the microstructures of alloys where tensile elongation is limited without changing the sample dimensions[86,91,92]. These induced large strains can lead to material failure. Therefore, depending on the type of material, the amount and accumulation of strains in the material should be reduced to avoid premature fracture[67,93,94]. Performing ECAP at room temperature can be tasking, due to ductility limitations of materials and/or high-pressure requirements. The process can, however, be performed at elevated temperatures, but this leads to large grain sizes and increased numbers of grain boundaries with low angle misorientations[86,90,95,96]. Performing ECAP using route B_C has been found to be the most effective in producing ultrafine grains with high angular grain boundaries (HAGB) [97,98]. Conventional ECAP was used to improve the mechanical strength of Mg-Al-Mn (AM70) alloy by Gopi et al[99] after 4 passes from an initial 133 MPa to 242 MPa due to grain boundary strengthening from the ultra-fine grains produced after ECAP pressing. AZ91D+Y magnesium alloy was processed via conventional ECAP processing by Zhao et al[100]. The ultimate tensile strength (UTS), yield strength (YS) and elongation to failure (Ef) increased pass by pass. ECAPed ZE41 magnesium alloy achieved significant improvement in YS from 160 MPa to 230 MPa and in ductility from 8% to 20%. In another study, Ding et al[101] reported that the formation of ultra-fine grains, dislocation slip and mechanical twinning are attributed to this improvement.

Research conducted on AZ61 magnesium alloy by Kim et al[102] also reported the reduction in grain size and increase in ductility after each successive ECAP pass. In another work, Gopi et al[103] also successfully improved the tensile strength and hardness of AM90 alloy by ~128% and 23%, respectively, when route B_C of ECAP was employed to process the alloy for 2 passes. Commercial cast AZ31 Mg alloy sheets were ECAPed at 225 °C via routes A, C and D with a channel angle of 110° by Suh et al[104]. The texture and mechanical properties of the alloy after ECAP were investigated. It is reported that ECAP effectively modifies the texture of the alloy as the direction of shear changes. Also, there is a decrease in YS as a result of the movement of the basal <*a*> slip. The mechanical properties of Mg-Zn-Ca-Mn alloy processed at 300 ° C by ECAP were successfully improved as investigated by Tong et al[105]. Dynamic recrystallization resulting in grain refinement contributs to the high YS of ~270 MPa and the refinement of the secondary grains leads to a good elongation of ~22.7%. The formation of strong basal textures after ECAP also contributes to the high YS.

1.2 Rotary die equal channel angular pressing (RD-ECAP)

Conventional ECAP, with its excellent achievement over years, still has drawbacks in processing hard-to-deform materials further to the nanoscale, relatively high production cost and reinserting the billet into the die for every ECAP pass performed[58,106]. Due to these limitations, a new processing system was developed known as rotary die equal channel angular pressing (RD-ECAP) [107-109], which solves these problems and achieves excellent and enhanced physical and mechanical properties[110,111]. The RD-ECAP system consists of four cylindrical channels, all converging in the center of the rotary die, with four punches inserted in each cylindrical channel, as depicted in Fig.4. The punch on the upper side of the billet has a portion of its length sticking out of the die on which the plunger presses the billet. The sample to be pressed is inserted in the center of the die with the punches securing it

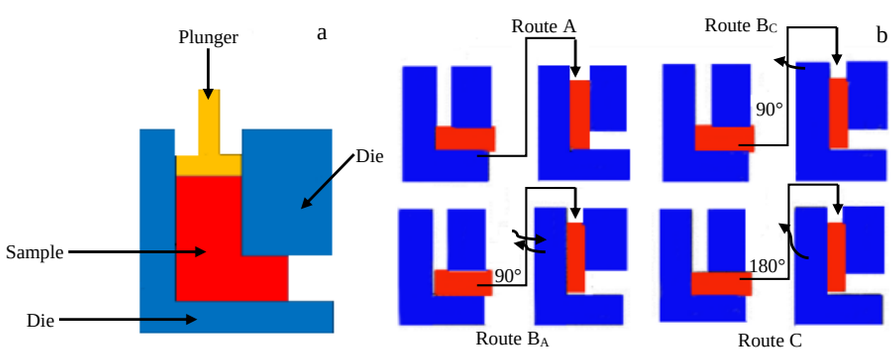

Fig.3 Typical conventional ECAP processing technique: (a) set-up and (b) pressing routes[85]

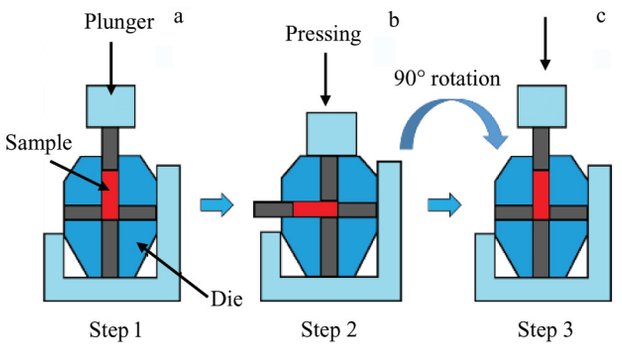

Fig.4 RD-ECAP processing technique: (a) initial set-up, (b) first pass, and (c) 90° rotation[112,113]

in place at all angles. The billet is extruded through the left horizontal channel after which the die rotates 90° clockwise for the next pressing. After each rotation, the die is returned to the initial configuration system with the exposed punch at the top, ready for the next pressing[114]. To perform the pressing at an elevated temperature, the entire die with the billet fastened with all four punches can be placed in a furnace held at the desired temperature and duration before returning to the hydraulic press for pressing. The strain induced during the RD-ECAP process is given by the equation:

$$\Delta\varepsilon = \frac{2N}{\sqrt{3}} \quad (2)$$

where N is the number of passes[112].

This method aside from being simple and reducing the processing time compared to the conventional method, also successfully improves the strength, ductility, and hardness of the processed sample. Nevertheless, compared to other techniques, the pressing is fixed at route A and 90° pressing angles. Comparatively, it has a small aspect ratio[90]. In another related work, Huang et al[115] observed and reported that complete dynamic recrystallization with an average grain size of 1.5 μm was obtained after pressing for 12 passes using the RD-ECAP setup. This resulted in a high UTS of 372 MPa and Ef of 8%. Also, research conducted by Xu et al[116] indicated that high strength and ductility with good plastic formability were obtained after AZ91 alloy was processed via RD-ECAP to produce ultra-fine grains with high Schmidt factor and homogenenous β-$Mg_{17}Al_{12}$ phases. A high strength of ~307 and ~322 MPa was obtained for the cast-ECAP and homogenized-ECAP samples, respectively; the elongation values also reach ~11.5% and ~19.6% respectively. A homogenous grain size with a high Schmidt factor was also observed after RD-ECAP of AZ91 performed by Xu er al[117]. The secondary phases dissolved and formed ultra-fine grains of 200~500 nm. Another investigation of AZ91 Mg alloy that was hot extruded and subsequently RD-ECAPed was conducted by Xu et al[118]. A simultaneous improvement in both strength and ductility of the processed alloy in three orthotropic directions was observed. Considerable anisotropy in the alloy was observed as the achieved YS was between 214.3 and 279.9 MPa, the UTS was between 321 and 382 MPa and the ductility was between 8.2% and 15.5% after 12 passes along the 3 tensile directions. Homogenous and equiaxed fine grains of ~7 μm were achieved after 4 passes, subsequently reaching ~6.9 μm after 12 passes. Both grain refinement strengthening and texture strengthening attributed to the improved mechanical properties. A ZE41A (4.9wt% Zn, 1.4wt% RE, 0.7wt% Zr) Mg alloy was also processed via RD-ECAP to achieve ultrafine grains of ~1.5 μm and a high strength of ~305 MPa after 32 passes, tested at room temperature by Ma et al[119]. The YS was ~290 MPa and the Ef was ~13% tested at room temperature. The occurrence of DRX was observed during the processing, resulting in homogenous and equiaxed ultrafine grains and benefiting the excellent strength and appreciable ductility. Also, a two stage RD-ECAP processing route was employed by Ma et al[120] to process Mg-5Zn-2Al-2Sn (ZAT522) alloy. The first stage was processed at 220 °C for 2 passes before subsequent 2 passes at 130 °C. Grain refinement of ~1.4 μm was achieved after the first stage pressing, reaching a yield strength of 245 MPa. Furthermore, the second pressing stage endowed the alloy a further refinement, reaching a grain size of ~1.18 μm, and a yield strength of ~335 MPa. An ultrafine grain structure of ~700 nm was also observed in the precipitate-rich region. The authors attributed the strength improvement to the combined effect of precipitation and grain boundary strengthening. RD-ECAP was employed by Wang et al[121] to improve the strength and ductility of Mg-3.7Al-1.8Ca-0.4Mn alloy. The RD-ECAP process effectively refined the grains and broke the network-shaped Al_2Ca phase. Uniformity of the Al_2Ca phase was observed with a decrease in temperature and an increase in number of passes. A high UTS of 354 MPa and Ef of 10.3% were achieved after processing the alloy at 300 °C for 12 passes. The refined DRX grains, and nanosized and refined precipitates contributed to the high strength achieved.

1.3 ECAP with parallel channels

Tubular channel angular pressing (TCAP) and parallel tubular channel angular pressing (PTCAP) are examples of ECAP processing techniques with parallel channels for producing UFG and nanostructured tubes[122,123]. Even though both processes are similar, TCAP is performed in a single pressing cycle, whereas PTCAP is performed in two half-cycles with relatively lower loads employed in the PTCAP process compared to the TCAP technique[124]. PTCAP also induces high strains in a single pass and achieves relatively better strain homogeneity throughout the tube thickness[125]. Employing this process for pressing is similar to processing via route C of the conventional ECAP process[125,126]. Fig. 5a and 5b show the schematic of typical TCAP and the processing parameters, respectively. The tubular sample is placed in the gap between the die and mandrel or inner and outer dies. The hollow punch on the upper side of the die is used to press the sample until it reaches its maximum tube diameter. This process ends one pressing cycle in TCAP and a half cycle in PTCAP. The second half cycle for PTCAP is performed similarly with a second punch performing the pressing for the lower side of the die. This pressing returns the

material to its initial dimensions. The cycles described for both processes can be repeated several times without changing the cross-sectional area of materials. The effective strain induced during parallel channel pressing is given by Eq.(3):

$$\varepsilon_{eq} = \frac{1}{\sqrt{3}}\left[2\cot\left(\frac{\phi}{2}+\frac{\psi}{2}\right)+\psi\,\mathrm{cosec}+\left(\frac{\phi}{2}+\frac{\psi}{2}\right)\right] \quad (3)$$

However, considering the radial and circumferential strain induced by the process, the total equivalent strain after a number of passes is given by Eq.(4):

$$\bar{\varepsilon}_{TN} = 2N\left\{\sum_{i=1}^{2}\left(\frac{1}{\sqrt{3}}\left(\left(2\cot\left(\frac{\phi}{2}+\frac{\psi}{2}\right)+\psi\,\mathrm{cosec}+\left(\frac{\phi}{2}+\frac{\psi}{2}\right)\right)\right)+\ln\frac{R}{R_0}\right)\right\} \quad (4)$$

where, N is the number of passes with the various parameters represented in Fig.5b[124,127].

Research conducted by Faraji et al[128] employed TCAP in processing AZ91 magnesium alloy. Excellent grain refinement of ~1.5 μm was achieved after a single pass as well as improved hardness homogeneity along with the tube thickness. The experimental and computational analysis conducted by Faraji and his team[129] also on AZ91 magnesium alloy achieved excellent grain refinement from an initial 150 μm to 1 μm which is a prerequisite for improvement in the mechanical properties of Mg alloys. The channel angle, friction coefficient and back pressure had a significant effect on the strain homogeneity observed. In another experiment, Mg-3Al-1Zn was processed at 300 ° C via PTCAP by Eftekhari et al[130]. The researchers reported the formation of a fine grained structures after multipass pressing. Bimodal microstructure with large grains after a single pass was replaced with a homogenous and refined microstructure with increase in number of passes. The highest Ef of ~281% was achieved after 4 passes, tested at a temperature of 450 °C. A UTS value of ~260 MPa was obtained after 4 passes, tested at room temperature. Fata et al[131] also processed Mg-9Al-1Zn alloy via PTCAP at 300 ° C for 3 passes. Significant grain refinement of 4 μm was achieved from an initial 150 μm in the as-cast state. The UTS value increased steadily after every successive pass, reaching a maximum value of ~300 MPa at room temperature after 2 passes whereas the 3 pass sample reached a value of ~200 MPa. The evolution of microcracks and voids in the 3 pass sample led to the reduction in strength. A high ductility of ~178% was achieved after the 2 pass sample was tested at 400 ° C. AZ31 Mg alloy was processed via multipass PTCAP and tensiled at various temperatures by Fata et al[132]. Successful ultrafine grain structure was achieved. The achieved results reported indicated a high Ef of 263% after 2 passes at a testing temperature of 400 °C. This is due to grain boundary sliding being the dominant deformation mechanism. Research conducted by Mesbah and his team[133] achieved successful ultrafine grains of 7~0.9 μm after processing ZK60 alloy via PTCAP at 300 ° C, and UTS, YS and Ef values of 397 MPa, 320 MPa and 14% were achieved, respectively. Dynamic recrystallization as well as the breakup and distribution of precipitates on the newly formed grains in the alloy structure were the dominant factors for achieved mechanical properties.

1.4 Incremental ECAP

During ECAP processing, high strain and increased frictional force are introduced, which serve as deterrent to its potential use in large size materials. To overcome this challenge, incremental shear during the ECAP process was developed, and successfully employed in processing large plates, sheets and bars[134]. In this process, the billet feeding/pressing stage and deformation stages are separated, resulting in a significant reduction in the feeding force, which is in contrast to the conventional ECAP method, where both stages occur simultaneously[135]. I-ECAP processing setup consists of a punch that reciprocates periodically and a die for incremental injection of the billet or material, as shown in Fig.6.

Feeding of the billet occurs when the punch is withdrawn by a distance, allowing the billet to be placed in a position shown in Fig.6 known as the pressing stage. Once the billet is in place without further movement, the punch presses the billet, forcing it through the output channel known as the deformation stage[138]. As long as the feeding stroke is small ("*a*" as shown in Fig.6), the resulting overlapping shear zones form uniform strain distribution along with the billet. Furthermore, to increase the efficiency of the process and to reduce friction, a double system was proposed, which works similarly to the single system. In another study, Gzyl et al[139] successfully produced UFG materials well below ~1 μm after processing AZ31B magnesium alloy by I-ECAP at 150 °C. A

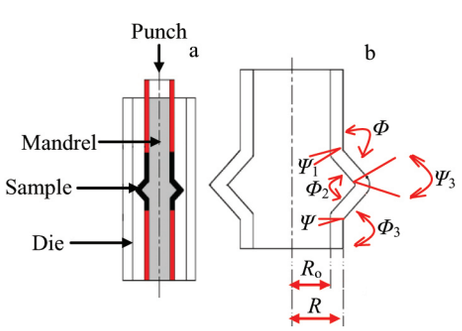

Fig.5 TCAP set up (a) and die parameters (b)[124,127,128]

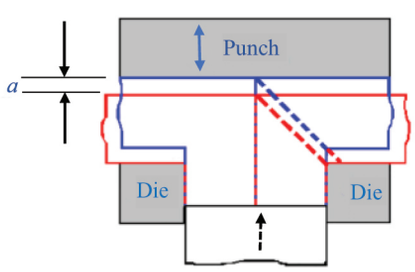

Fig.6 Schematic of an I-ECAP process[136,137]

300 MPa YS with simultaneous ductility improvement was achieved after 4 passes. AZ31B was I-ECAP processed again via route A and B_C by Gzyl and his team[137]. UFG was achieved in both routes with route A, obtaining a higher tensile strength compared to route B_C without a decrease in ductility. Another study on the mechanical properties and microstructure of AZ31B Mg alloy processed via I-ECAP for 4 passes was conducted by Gzyl et al[140]. The pressing was done in three different routes (A, B_C and C) at 250 °C. The processed alloy microstructure was reported to form homogenous and refined grains of ~5 μm in all three processing routes. The true stress values for routes A and B_C were reported to be 290±5 MPa whereas the true stress value for route C was decreased to 262 MPa. The true strain values were also reported to be between ~0.14 and ~0.21% for all three processing routes. The investigation highlighted that the grain size of the alloy was not affected by the processing route but significantly changed the mechanical properties. Texture was highlighted as a major contributory factor for controlling the mechanical properties of AZ31B alloy at room temperature, processed via I-ECAP followed by heat treatment, investigated by another research conducted by Gzyl and his team[141]. The investigation was conducted for 4 passes via route A and C. Grain size reduction of ~2.5 μm was achieved for both routes, increasing the strength of the alloy pressed via route A to 205 MPa, conducted at 250 ° C. Ductility enhancement via route C after I-ECAP plus annealing at 250 °C was obtained, attaining a value of 0.35 true strain which was attributed to the basal slip, texture development and homogenization of the grains after heat treatment. A yield strength of 300 MPa was also achieved at 150 ° C via route A. The formability of AZ31B was investigated in a research conducted by Gzyl et al[142]. I-ECAP was employed via different routes and processing temperatures. The investigation reported strong influence of initial microstructures on the optimum processing temperature. Fine grains of ~8 μm were successfully achieved at 200 °C while coarse grains of ~60 μm were obtained after processing at 250 °C. The research highlighted that route C is the most susceptible to fracture while route A allows processing at a temperature of 150 °C.

1.5 Equal channel angular rolling (ECAR)

Conventional ECAP process has a limited application in industrial production since it is a discontinuous process. Therefore, ECAR was developed to address this deficiency by producing continuous and long metal sheets[143]. The process induces large strains to metals without change in the cross-sectional area[144]. In equal channel angular rolling, the metal to be pressed is fed into the die by the surface friction between the rollers (guide and feeding rolls) and the metal surface as opposed to the pressure exerted by the punch on the metal in the conventional method[145]. Therefore, the rolling contact area, the friction coefficient and ratio of rolling can affect the overall power exerted during the pressing process. The cross-sectional area of the input channel is designed smaller than the output channel to reduce the frictional force during the process[145]. Fig.7 shows a typical ECAR setup.

AZ31 magnesium alloy was subjected to ECAR for 8 passes, as investigated by Hassani et al[147]. Significant ultra-fine grains with an average grain size of 3.9 μm were achieved. Significant ductility enhancement and strain hardening were observed as a result of texture softening and grain refinement from the ECAR process. The Ef was observed to improve from an initial 8% to 19% after 2 passes. The drawability of the AZ31 alloy processed by ECAR was also investigated by Cheng et al[148] whose findings pointed out successful improvement in ductility as a result of crystal orientation change, inducing several deformation mechanisms in the alloy. The drawability ratio of the alloy was observed to improve from an intial 1.2 to 1.6 at room temperature. Chen et al[149] also indicated that due to a crystal orientation change from basal to non-basal in the ECAR process, the processed AZ31 magnesium alloy achieved lower yield strength and higher ductility with increasing number of passes at ambient temperature. The Erichsen value was reported to improve from 4.18 to 6.26 after 4 passes of ECAR, resulting in an increase in the drawability ratio of the alloy at room temperature from 1.2 to 1.6. Grain refinement of AZ31 magnesium alloy was achieved when Hassani et al[150]. Processed the alloy by multipass ECAR at elevated temperatures. Nano grains with an average size of 32 nm was achieved after 10 passes with significant ductility improvement resulting from the activation of non-basal planes. The hardness of the alloy was increased by 53% after 8 passes. Another AZ31 Mg alloy was processed via equal channel angular rolling and continuous bending (ECAR-CB) by Shi et al[151]. The authors highlighted that extension twins (as a result of the introduction of basal and prismatic textures) were observed which increased with increasing temperature, due to the coarse grains and increased grain boundary migration. Complete recrystallization at different final rolling temperatures was also observed. However, increasing the final rolling temperature benefited the increase in plasticity and formability of the alloy. The highest Ef of 26.1±2.1% was achieved at a final rolling temperature of 550 °C whereas the highest UTS of 225±11 MPa was achieved at a final rolling temperature of 350 ° C. Room temperature formability was achieved by preheating AZ31 Mg alloy at 400 °C for 3 min followed by processing via ECAR, conducted by Cheng et al[152]. The grain size of the rolled sample was ~10.5 μm,

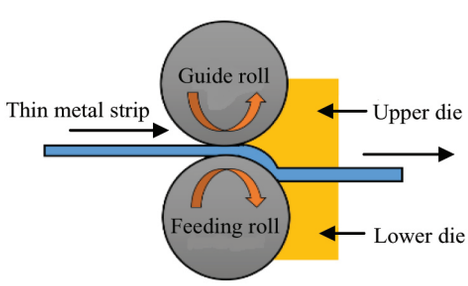

Fig.7 Schematic of an ECAR process [146]

comparatively equal to the initial grain size of ~11.3 μm of the as-cast sample. A high strength of ~300 MPa and ductility of ~0.12% was achieved, attributed to the introduction of large amounts of twins during the ECAR process. ECAR for 4 passes was employed by Cheng et al[153] to process AZ31. The pressed sheets were preheated at 450 °C for 5 min, prior to each rolling pass. The UTS of the processed alloy of ~250 MPa was not significantly changed compared to the as-cast state. However, the ductility was significantly improved, reaching a value of ~24%. The observed low strength was attributed to the coarse grains and unfavourable orientation of the basal plane for slipping while the improved ductility was attributed to the modification of the crystal orientation.

2 Influencing Factors

2.1 Influence of number of passes

During ECAP processing, there is a reduction in grain size of the alloy processed after each pass, and this reduction in grain size is an important strengthening mechanism resulting in the improved strength of the ECAPed processed alloy[154]. Although the physical and mechanical properties of metals are determined by several factors, the grain size of metal has an important effect on the mechanical properties of the alloy. ECAP induces strains into the phase structure of the alloy, transforming the grain cells to sub grains and then to high angular grain boundaries (HAGB)[154-156]. The pass number of the ECAP method is directly proportional to the increase in the number of HAGB and inversely proportional to the misorientations and spacing between HAGB[157,158]. Boundary (grain and subgrain) strengthening or hardening is also a major strengthening mechanism for the ECAP process[159]. An excellent SPD processing technique should be capable of producing high angle grain boundaries in the material, bringing material property changes[58,160]. The grain size is directly related to the strength of the alloy by the famous Hall-Petch equation. It is the governing equation for the effect of grain size on a metal's properties. From the Hall-Petch equation, it is known that the strength of the metal/alloy increases with a decrease in the grain size of the alloy[161-164], which is stated as:

$$\sigma_y = \sigma_0 + k_y d^{-\frac{1}{2}} \quad (5)$$

where σ_0 is friction stress, d is average grain diameter and k_y is constant of yielding. σ_0 and k_y are constants varying from metal to metal. Microstructural inhomogeneity is a natural phenomenon occurring during the SPD processing of hcp materials[60,91,165]. Fig. 8 shows typical electron back-scattered diffraction (EBSD) images, illustrating the microstructural evolutions of Mg processed by ECAP. Research has also shown that grain refinement of Mg alloys is somewhat complex, with the formation of either homogenous or bimodal grain structures after ECAP[166,167].

Also, during the strengthening of Mg-alloys, as the grain size reduces, resistance to twinning increases appreciably as compared to dislocation slip, becoming more challenging to deal with above aspecific critical grain size[168]. The

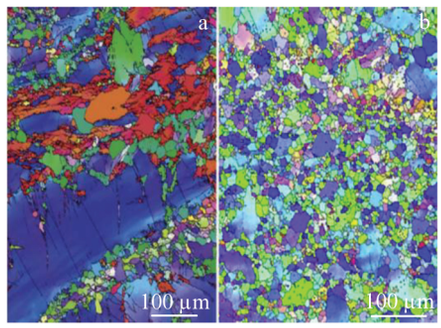

Fig.8 EBSD microstructural images of single crystal Mg after 1 pass ECAP (a) and polycrystalline Mg after 4 passes ECAP (b)[60,91,165]

mechanical properties of Mg-9Li alloy were also improved via RD-ECAP in our previous work[169]. The mechanical performance of the alloy after every successive 4, 8, and 16 ECAP pass was investigated. The initial ultimate tensile strength (UTS) and yield strength (YS) of the as-cast alloy were 102 and 52 MPa, respectively. A successful improvement in the UTS and YTS was obtained, reaching 106 and 88 MPa after 4 passes, 133 and 110 MPa after 8 passes and 116 and 100 MPa after 16 passes, respectively. A reduction in grain size of the α-Mg phase to ~2 μm after 8 passes was observed, as indicated in the transmission electron microscope (TEM) image in Fig.9.

A combination of grain boundary strengthening and dislocation strengthening of both α-Mg and β-Li phases were the major contributory factors to the improved strength properties observed[170,171]. The formation of HAGB was also reported by Yang et al[172] as a contributory factor to the improved mechanical properties of Mg-3%Li-1%Sc after 4 passes of ECAP process.

ECAP was employed by Minárik et al[173] on LAE442 magnesium alloy to improve the YS, UTS and Ef. The process was conducted for 12 passes with a gradual increase in mechanical properties after each pass. A grain size reduction from an initial ~21 μm to ~11 μm was achieved after a single pass. Further reductions to ~6 and ~2.6 μm were achieved after 2 and 4 passes, respectively. After 8 and 12 passes, the grain size was observed to be ~1.9 and ~1.5 μm, respectively.

Fig.9 TEM image of α-Mg phase in ECAPed 8 pass Mg-9Li alloy[169]

Successful improvements in the YS, UTS and Ef were observed from initial values of 142 MPa, 149 MPa and 0.4% to 193 MPa, 218 MPa and 0.8% after 4 passes, respectively; the mechanical properties finally reached values of 192 MPa, 221 MPa and 1.0% after 12 passes, respectively. The substantial grain refinement improved the YS and UTS as well as the changes in fracture mechanism, combining the effect of low angle grain boundary (LAGB) fraction decrease and the total grain boundary volume fraction increase[174-176]. Research conducted by Liu et al[177] on Mg-8%Li-1%Al for 4 passes at a temperature of 130 °C via route A, indicated an increase in mechanical properties after every successive pass, as illustrated in Fig. 10. However, Ef after one pass ECAP is decreased significantly, from 36% to 12% but subsequently increased with increase in the number of passes.

The refinement of both the α-Mg and β-Li phases, and formation of equiaxed and homogenous microstructures, as depicted in the TEM images in Fig. 11[177], contribute extensively to the improved mechanical properties. The researchers also ascribed the increase in strength with a decrease in Ef after one ECAP pass to the induced massive internal stress coupled with saturated dislocations from the process[178,179].

2.2 Influence of processing temperature

A wealth of ECAP studies on Mg alloys have been focused on its application at higher temperatures due to the limited formability capability of HCP crystal systems[119,180,181]. The structural and thermal stability of the alloy is an essential factor in improving the mechanical properties of the alloy, especially its ductility[182,183]. Grain refinement is generally accepted to occur due to recovery processes known as continuous dynamic recrystallization (cDRX) or geometric dynamic recrystallization (gDRX). The former (cDRX), occurs when there is the formation of high angle grain boundaries (HAGB) due to grains forming cells as well as subgrains. The latter (gDRX), occurs when grain boundaries (normally serrated) from the SPD process meet, resulting in finer grain formation[85,184-186]. Both grain growth and dynamic recrystallization (DRX) occur simultaneously at higher ECAP temperatures, forming coarser grains as compared to the processing at lower temperatures[187]. In our previous work[169], RD-ECAP was performed at a heating temperature of 200 °C for 30 min before pressing for 4 and 8 passes. The 16-pass pressing was conducted with a 30-min reinsertion of the die into the furnace after 8 pass pressing, before completing the final 8 passes. A steady increase in mechanical properties was observed with an increase in the number of passes. However, due to the coarsening of the grains and softening of the alloy after processing of the 16-pass sample, the UTS and YTS decreased with an increase in Ef as compared to the 8-pass sample. After successfully performing ECAP at 403 K, which is below the melting temperature (T_m) of the alloy (Mg-8%Li-1%Al) by Liu and his team[177], it was concluded that there is no evidence of recrystallization during the ECAP processing, as indicated by the observed TEM micrographs. Due to this, the influence of the HAGB led to an increase in the strength properties of the alloy. The room temperature strength improvement with a reduction in ductility of various Mg-Li-Zn alloys was achieved when ECAE was employed by Chang et al[180]. The superplastic properties of the Mg-Li-Zn alloys were, however, improved at elevated temperatures. The mechanical properties of the alloy with 9wt% Li and processed via route C at 100 and 150 °C are summarized in Fig.12.

2.3 Influence of processing route

The processing route also plays a vital role in obtaining particular textures and microstructure[188-190] and influences the crystal structure of Mg-Li alloys[191,192]. Studies have shown that ECAP processing of Mg-Li alloys results alignment of the basal planes along the normal direction of pressing[193,194]. Magnesium alloys have three basic slip systems (<*a*>basal, <*a*> prismatic and <*c*+*a*> pyramidal), and only the basal slip system dominates[195]. However, during ECAP processing, the strain path changes after each pass, forming equiaxed grains, activating new and active slip systems and getting rid of dislocations to increase cell boundary misorientation[158].

ECAP also induces strong deformation textures, which is an important aspect of the improvement mechanism in the mechanical behaviour of Mg alloys, persisting even after recrystallization[196-198]. Texture strengthening has been

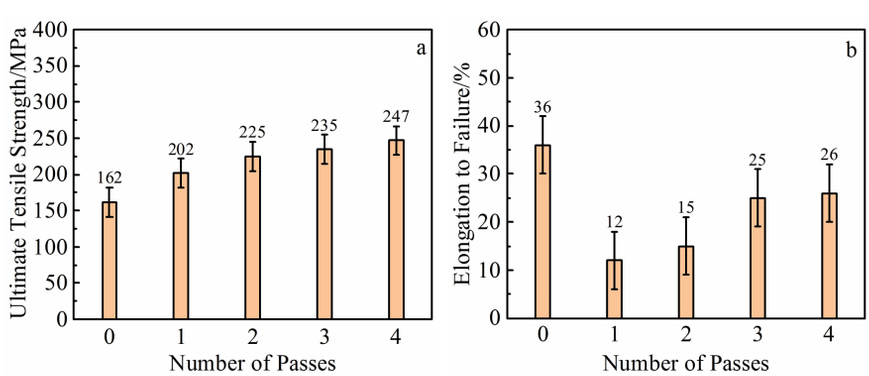

Fig.10 Mechanical property values of Mg-8%Li-1%Al alloy processed at 130 °C via route A at different ECAP passes: (a) tensile strength and (b) ductility [177]

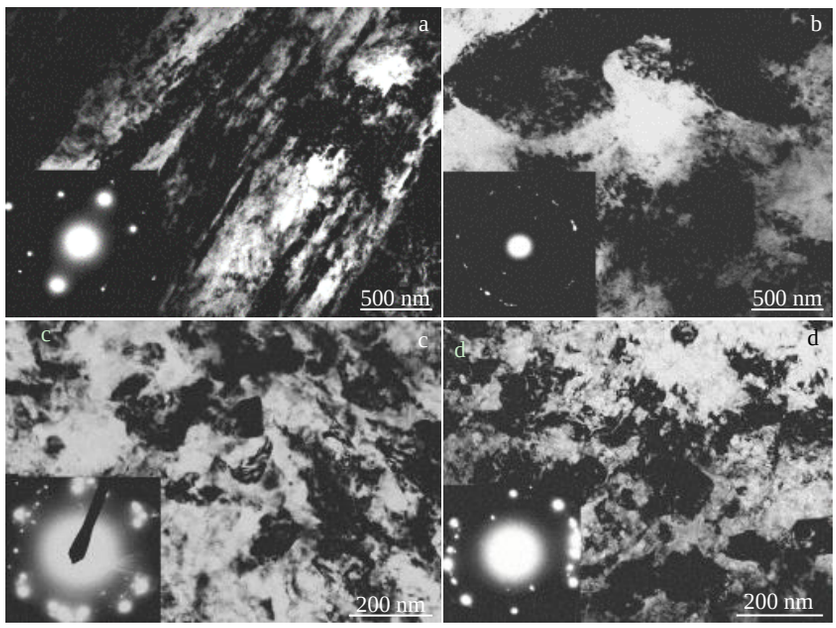

Fig.11 TEM micrographs of α phase after 1 pass (a) and 4 passes (b); β phase after 1 pass (c) and 4 passes (d)[177]

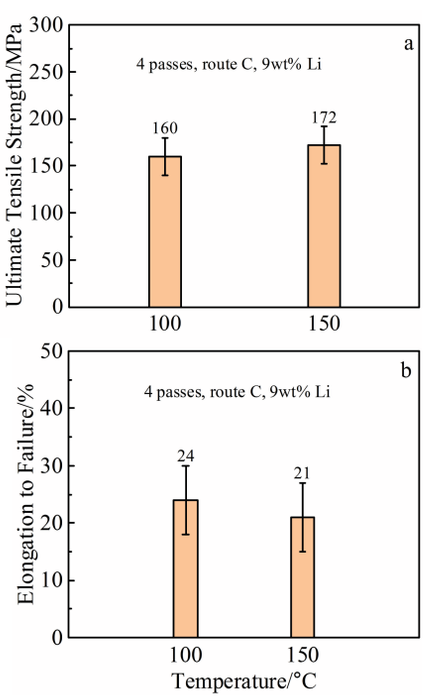

Fig.12 Mechanical property values of LZM910 and LZAM9110 after ECAP processing at 100 °C and 150 °C for 4 passes via route C: (a) ultimate tensile strength and (b) ductility[181]

acknowledged by several researchers[199,200] as an important strengthening mechanism that ECAP introduces when employed. An investigation conducted by Liu et al[201] showed an improvement in the mechanical property of Mg-3.3%Li alloy subjected to ECAP processing conducted at 250 ° C through two separate processing routes, A and B_C. A total of 4 passes were conducted for each processing route. The results indicated an improvement in the YS value for both route A and route B_C from an initial ~58 MPa to ~88 and ~65 MPa, respectively. The UTS was also observed to improve from an initial ~125 MPa to ~156 and ~145 MPa for route A and B_C, respectively. The Ef value also improved from an initial ~20% to ~28% and ~45% for routes A and B_C, respectively, as depicted in Fig. 13. Grain refinement and extremely strong textures were reported for samples processed via both routes. However, partial recrystallization occurred via route A while total recrystallization occurred via route B_C. Strong basal textures were also formed when Mg-3%Li-1%Sc was ECAPed via route B_C by Yang et al[172]. Their team conducted a 4 pass ECAP process and reported a substantial improvement in the strength properties of the alloy. The YS increased from an initial 60.2 MPa to 126.8 MPa, whereas the UTS also increased from an initial 135.3 MPa to 194.3 MPa; this represented a 110% and 44% increase in the YS and UTS values, respectively, after the 4-pass ECAP. The Ef was almost unchanged. The formation of HAGB and strong basal texture are attributed to the obtained result indicated by the researchers. Research conducted by Karami and his team[202] on LZ121 and LZ61 magnesium alloys, processed by extrusion and ECAP at 200 ° C under the route B_C, was understudied. Results of the experiment confirmed an increase in YS from 84 MPa in the extruded state to 113 MPa after ECAP for LZ121. The UTS after ECAP reached a value of 119 MPa from an initial 113 MPa after extrusion. This is mainly due to grain refinement. However, with an increase in the Li content of the Mg-Li alloy, the crystal lattice axis ratio (c/a) of the hcp α-phase reduced so that slipping between the crystal phases was relatively easier[202,203].

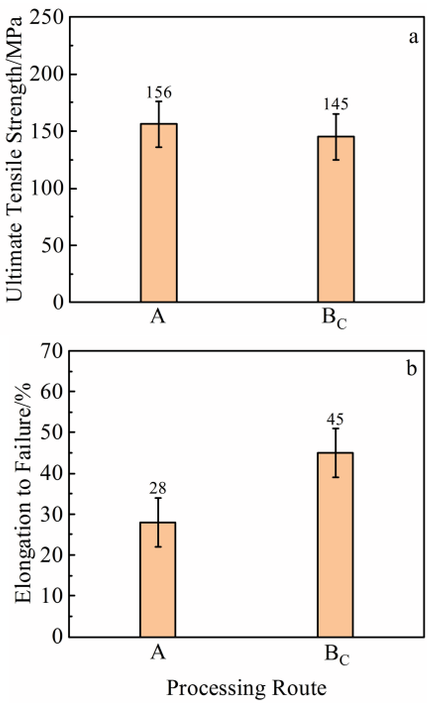

Fig.13 Mechanical property values of 4-pass ECAP processed Mg-3.3%Li via route A and B_C performed at 250 °C: (a) ultimate tensile strength and (b) ductility [201]

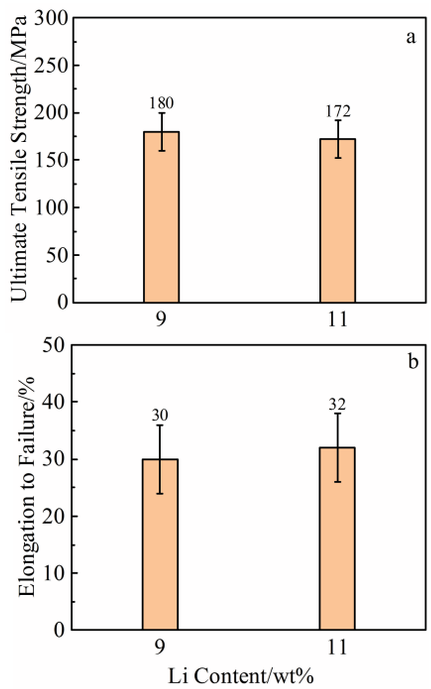

Fig.14 Mechanical property values of 4-pass ECAP processed LZ91 and LZ11 via route B_C performed at 100 °C: (a) ultimate tensile strength and (b) ductility[181]

3 Influence of Li Content

Li is considered the lightest metal with a density of ~0.533 g·cm^{-3} [204]. Li reduces the density of the overall alloy with a small amount, improving the room temperature ductility and deformability of the α-Mg (hcp). This is as a result of the reduced lattice constant ratio (c/a) when the Li atoms serve as substitutional atoms for the Mg atoms in the atomic structure of the alloy, resulting in crystal structure alteration from hcp to bcc[205-209]. The critical resolved shear stress (CRSS) for pyramidal slip is also lowered at lower temperatures when Li is solid solution alloyed with Mg[210]. Due to the fewer number of active slip systems in Mg and its alloys, plastic deformation is a challenge. However, at elevated temperatures, there is the activation of more slip systems, which facilitates better plastic deformation of the alloy[211]. In our previous work[169], it was outlined that dynamic recrystallization takes place preferentially in the β-Li phase of Mg-9Li alloy after ECAP processing, leading to limited strengthening and potentially softening of the alloy. Various Mg-Li alloys with varying Li content were investigated by Chang et al[181], and the obtained mechanical property values are summarized in Fig.14.

The authors acknowledged that the alloy containing a high percentage of Li (11wt%) was weaker compared to alloy containing 9wt% Li due to the higher percentages of weak β phase in the as-cast state. After ECAP, the samples with higher Li content obtained relatively lower UTS, YS and microhardness of both α and β phases. However, Ef was relatively improved. The mechanical behaviour of Mg-6Li-1Zn (LZ61) and Mg-12-1Zn (LZ121) alloys processed via ECAP by Karami et al[202] was investigated. The research achieved higher UTS and YS values of ~188 and ~137 MPa, respectively for the processed LZ61 alloy compared to LZ121, which obtained UTS and YS values of ~119 and ~111 MPa, respectively. The percentage of Li content in both alloys plays a significant role in mechanical property values. The effect of Li content on the microstructures and mechanical properties of Mg-Li alloys was investigated by Zhao et al[212]. Li addition was reported to increase the grain size of the alloy due to DRX and increased prismatic slip. The study showed an increase in ductility with increase in Li content, and a decrease in YS and UTS with increase in Li content.

4 Influence of Microstructure

ECAP transforms the microstructure of alloy, usually producing ultrafine grained structures which ultimately lead to the improvement in the overall mechanical property. Microstructural change is therefore very important in influencing the mechanical property of Mg-Li alloys[173]. As discussed previously in Fig.2, the phase diagram of cast Mg-Li alloys show three distinct crystal structures at room temperature depending on the Li content concentration. The single hcp α-phase exists below 5.5wt% Li and has a comparatively higher strength and low formability due to the limited number of slip systems. The duplex α+β phase formed between 5.5wt% and 10.2wt% Li content consists of both hcp α-Mg and softer bcc β-Li phase, having a combination of moderate strength and ductility. Alternatively, the single bcc β-Li phase existing above 10.2wt% Li content has a higher formability and lower strength due to the existence of softer

bcc β-phase[53,175,213]. The processing of Mg-Li alloys can be employed at various temperatures while due to the microstructural instability of Mg-Li alloys below 100 °C as a result of overaging, early studies proposed the necessity for developing Mg-Li alloys at elevated temperatures. Hence, various thermomechanical research processes on Mg-Li alloys such as ECAP, process the alloys at elevated temperatures [214]. Dutkiewicz et al [215] observed that the Mg-Li alloys with a dual phase structure show higher non-homogeneity after the first ECAP pressing compared to the single α-Mg phase alloys due to the relatively easier deformation, as a result of higher fractions of softer bcc phases and LAGB. Additionally, higher hardness and yield strength for the dual phase (Mg-9wt%Li-1.5wt%Al) alloy compared to the single α-phase Mg-Li alloy (Mg-4.5wt% Li-1wt% Al) was observed. Liu et al[177] also revealed that ECAP refines the grains of the original dual phase of Mg-8%Li-1%Al from the original coarse structure to refined grains, becoming more homogeneous and equiaxed after each successive pass. The authors stated that the initial grain size of the α-Mg phase (25 μm) was refined to 1~5 μm after the first pass, having a heterogeneous and non-equiaxed structure. The grains were further refined after 4 passes, reaching ~500 nm grain sizes which were homogeneous and equiaxed. Alternatively, the initial grain size of β-Li (18 μm) was also refined to ~200 nm after 4 passes, with homogeneous phases. Inhomogeneous deformation morphologies inside the β-phase after 1 pass ECAP show that {110}<111> slip is the dominating deformation inherent in the β-phase after the process[64]. The refinement in both the α-Mg and β-Li phases is shown in the TEM micrograph in Fig. 11. The effective grain refinement reflects an increase in strength to ~198 MPa, evidently as a result of grain refinement, grain boundary and dislocation strengthening. Also, single α-Mg phase containing 3.3wt% Li was processed at 523 K via route A and B_C pressing by Liu et al[201]. The grain refinement and development of textures significantly improve the mechanical properties of the alloy. The investigation highlighted the occurrence of recrystallization after ECAP, which is evident from the TEM micrographs shown in Fig.15.

However, the extent of recrystallization and the microstructural features defer to the number of passes, processing route and pressing temperature. Partial recrystallization occurred in the pressed route A sample, forming recrystallized grains in the range between 1.2 μm to 6 μm. Complete recrystallization occurred in route B_C sample with homogeneous and equiaxed grains having an average grain size of 3.4 μm. The observed texture and TEM micrographs showed that ECAP not only refines the microstructures but also introduces different texture components in the alloy, leading to improvement in the mechanical properties. Basal slip deformation also occurred at room temperature. Higher yield strength was achieved due to higher CRSS of the prismatic and <*c*+*a*> slips compared to basal slip. In the route A sample, more activity to induce deformation movement was observed in the prismatic and <*c*+*a*> slips compared to the basal slip. Karami et al[216] also processed three Mg-Li alloys (Mg-6Li-1Zn, Mg-8Li-1Zn and Mg-12Li-1Zn) via ECAP at 200 °C for 4 passes. Both Mg-6Li-1Zn (LZ61) and Mg-8Li-1Zn (LZ81) have a dual phase structure while the Mg-12Li-1Zn (LZ121) has a single β phase structure. Continuous dynamic recovery and recrystallization (CDRR) resulting in homogeneous and refined grains were observed for LZ61 and LZ121 alloys after the pressing. However for the LZ81 alloy, due to the loss of Li after 4 passes, the grain size and volume fraction of the α-phase increased, reducing the grain refinement effect of the ECAP process. The observed/induced basal textures after ECAP for LZ61 and LZ81 alloys were inclined at 45° to the extrusion direction. However, the increased volume fraction of the β-phase in the LZ81 compared to the LZ61 alloy decreased the intensity of both basal and prismatic planes after ECAP. Alternatively, increasing the number of ECAP passes for the LZ121 alloy randomized the textures observed. The observed grain refinement and texture evolution resulted in an increase in UTS and YS. From the highlighted research conducted, the microstructural and grain refinement, leading to grain boundary and dislocation strengthening, is a major contributory factor to the observed strengthening of Mg-Li alloys processed by ECAP. Additionally, research has also shown that strong basal textures are formed after ECAP. For both deformed and recrystallized grains, the texture may be the same; however, there may be differences in the texture intensity[172]. This development and strengthening of texture after ECAP is therefore another important factor contributing

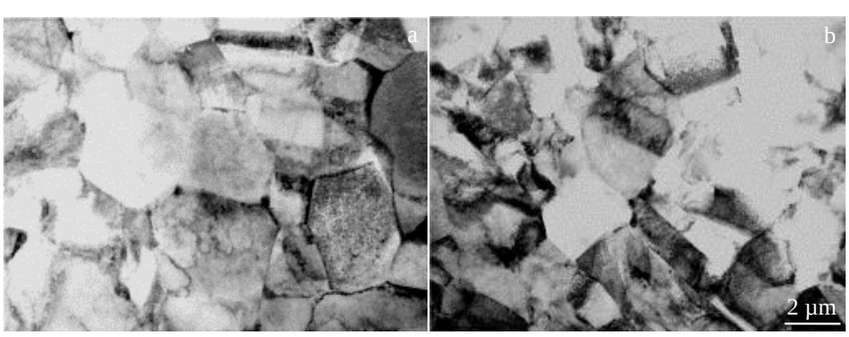

Fig.15 TEM micrographs of recrystallized grains after ECAP via route A (a) and route B_c (b)[201]

to the improved mechanical properties induced after ECAP. Summary of the principles, advantage, limitations and appliations of various types of ECAP is shown in Table 2, while summary of the mechanical properties of various Mg-Li alloys precessed via ECAP is shown in Table 3.

Table 2 Summary of the principles, advantages, limitations and applications of various types of ECAP

ECAP type	Principle	Advantage	Limitation	Application
Conventional	The metal is pressed by a plunger into a die	Simple and easy to operate; improving strength with good ductility	High production cost; billets have to be reinserted into the die for each pass	Metal rods and bars
RD-ECAP	The channels intersect at 90°, deforming the metal from both sides with a plunger	Simple and easy to operate; shortening time for operation; improving strength, ductility, and hardness	Complex deformation; only short billets produced at a time	Metal rods and bars
I-ECAP	The metal is incrementally injected into the die and pressed by a plunger	Reducing high strain and high frictional force	Limited length of billets produced	Large plates, sheets, and bars
Parallel channels	The metal is pressed between parallel channels	Total strain induced is homogeneous; reducing number of passes	Requiring manual processing	Cylindrical tubes
ECAR	Thin metal sheet is fed by rollers in ECAP channels. Sample is pressed by both rollers and die	Reducing strain	Metal length reduces after each pass	Long metal strips

Table 3 Summary of the mechanical properties of various Mg-Li alloys processed via ECAP

Material	Processing type	Process parameters			Li Content/ wt%	Mechanical properties			Finding/Remark	Ref.
		Pass No.	Temperature/ °C	Route		YS/ MPa	UTS/ MPa	EL/ %		
Mg-3.3%Li	Conventional extrusion+ECAP	4	250	A	3.3	88	156	28	Partial recrystallization was observed	[201]
Mg-3.3%Li	Conventional extrusion+ECAP	4	250	B_C	3.3	65	145	45	Total recrystallization was observed	[201]
Mg-9%Li	RD-ECAP	4	250	A	9	88	106	25	Improved strength properties as grains are refined	[169]
Mg-9%Li	RD-ECAP	8	250	A	9	110	133	24	The highest mechanical properties were obtained for this research	[169]
Mg-9%Li	RD-ECAP	16	250	A	9	100	116	31	Softening of the alloy due to reheating results in lower obtained strength properties	[169]

Continued Table 3

Material	Processing type	Process parameters			Li Content/ wt%	Mechanical properties			Finding/Remark	Ref.
		Pass No.	Temperature/ °C	Route		YS/ MPa	UTS/ MPa	EL/ %		
Mg-3%Li-1%Sc	Conventional ECAP	4	180	B_C	3	126.8	194.3	14.3	~65% deformation and ~35% recrystallized regions were observed after 4 passes. Strong basal textures were also obtained	[172]
Mg-8%Li-1%Al	Homogenization of ingots at 623 K for 24 h+conventional extrusion at 573 K +ECAP	1	130	A	8	169	202	12	The alloy strength was improved after 1 pass but ductility was reduced substantially	[177]
Mg-8%Li-1%Al	Homogenization of ingots at 623 K for 24 h+conventional extrusion at 573 K +ECAP	2	130	A	8	185	225	15	The strength and ductility increased after 2 passes	[177]
Mg-8%Li-1%Al	Homogenization of ingots at 623 K for 24 h+conventional extrusion at 573 K +ECAP	3	130	A	8	197	235	25	The strength and ductility increased after 3 passes	[177]
Mg-8%Li-1%Al	Homogenization of ingots at 623 K for 24 h+conventional extrusion at 573 K +ECAP	4	130	A	8	198	247	26	The strength increased substantially with improved ductility after 4 passes	[177]
LAE442	Extrusion at 350 °C+conventional ECAP	1	230	B_C	4	175±4	199 ± 3	0.9 ± 0.1	The mechanical properties increased after a single pass	[173]
LAE442	Extrusion at 350 °C+conventional ECAP	2	230	B_C	4	182±7	205 ± 8	0.9 ± 0.2	No further improvement in ductility was obtained	[173]
LAE442	Extrusion at 350 °C+conventional ECAP	4	230	B_C	4	193±6	218±6	0.8 ± 0.1	Grains became finer with decrease in ductility	[173]
LAE442	Extrusion at 350 °C+conventional ECAP	8	230	B_C	4	191±4	219±3	0.9 ± 0.1	Finer grains with steady mechanical properties	[173]
LAE442	Extrusion at 350 °C+conventional ECAP	12	230	B_C	4	192±4	221±4	1.0 ± 0.1	The mechanical properties were the highest after 12 passes	[173]

Continued Table 3

Material	Processing type	Process parameters			Li Content/ wt%	Mechanical properties			Finding/Remark	Ref.
		Pass No.	Temperature/ °C	Route		YS/ MPa	UTS/ MPa	EL/ %		
LZ61	Extrusion at 300 °C+conventional ECAP	4	200	B_C	6	137±2.5	188±3.6	42	The rotation of the basal plane by 45° resulted in lower mechanical properties of the ECAPed sample compared to the extruded sample	[202]
LZ121	Extrusion at 300 °C+conventional ECAP	4	200	B_C	12	111±1.9	119±2.1	30	Strength and ductility enhancement were attributed to grain refinement	[202]
LZ91	Conventional ECAP	4	100	B_C	9	160	180	30	Containing less weak β-Li phase resulted in better mechanical properties	[181]
LZ111	Conventional ECAP	4	100	B_C	11	150	172	32	Containing more weaker β-Li phase resulted in lower mechanical properties	[181]
LZM910	Conventional ECAP	4	100	C	9	140	160	21	Being weak to medium textures were observed	[181]
LZAM9110	Conventional ECAP	4	150	C	9	140	172	24	Being weak to medium textures were observed	[181]
LAZM9310	Conventional ECAP	4	174	C	9	130	172	25	Approximately higher microhardness of both α and β phases were obtained	[181]

5 Summary and Recommended Research Directions

Mg-Li alloys are of tremendous importance today. It is spanning from their widespread application in aerospace and automobile industries to biomedical and orthopedic applications. The need to grow and improve their performance in service is very crucial. ECAP as a severe plastic deformation technique has been identified as a processing technique of significant importance to the improvement in the mechanical properties of Mg-Li alloys from the researches highlighted in this paper, owing to the ultra-fine grains produced in addition to the grain boundary, dislocation and texture strengthening induced in the metal structure. However, studies have seldom been conducted via ECAP in strengthening Mg-Li alloys compared to other Mg alloys.

From the highlighted published works on Mg-Li alloys, the main ECAP parameters that affect the mechanical properties of the alloy are the number of ECAP passes, processing temperature, processing route, Li content and microstructural change. This study highlights that increasing the number ECAP passes directly increases the UTS and YS with appreciable ductility by reducing the grain size and forming UFG and HAGB. Ease of formability with improved strength and appreciable ductility is also observed when processed at elevated temperatures with the influence of dynamic recrystallization. ECAP also induces strong deformation and basal textures of which route B_C is the most effective in producing UFG and HAGB for mechanical property improvement of the Mg-Li alloys. The alloys with high Li content also play an essential role in improving alloys superplasticity. The microstructural alteration from coarse grains to refined and ultrafine grains after ECAP also improves the mechanical properties of the alloy.

Based on the highlighted parameters that affect the overall mechanical properties of the Mg-Li alloys, future studies can focus on combining, processing the alloy at temperatures between 150 and 250 °C, employing route B_C and more ECAP passes (8 and above) to effectively improve the mechanical properties of the alloy. Also, the die channel angle, which is an important parameter in influencing the total strain induced in the metal alloy, and ultimately the formation of UFG have been explored by some researchers. However, significant work has seldom been conducted to correlate the effect the die angle on the mechanical properties of Mg-Li alloys. Future research can be directed in this light, combined with different process parameters already explored to improve the mechanical properties of Mg-Li alloys. During the ECAP

process, the pressing speed or ram speed can be altered. This alteration affects the grain refinement of the alloy. Till date, the specific effect of the ram speed on the mechanical properties of Mg-Li alloys remains unknown. This research direction is where that future studies can be engaged in and may achieve some noticeable results.

References

1 Yaroshevsky A A. *Geochemistry International*[J], 2006, 44(1): 54

2 Nie Jianfeng. *Metallurgical and Materials Transactions A*[J], 2012, 43A(11): 3891

3 Xin Y, Hu T, Chu P K. *Acta Biomaterialia*[J], 2011, 7(4): 1452

4 Wong Wai Leong Eugene, Gupta Mamoj. *NanoWorld Journal*[J], 2016, 4(2): 78

5 Kim W J, Kim M J, Wang J Y. *Materials Science and Engineering A*[J], 2009, 516: 17

6 Sandlobes S, Friák M, Zaefferer S *et al. Acta Materialia*[J], 2012, 60: 3011

7 Yoo M H, Morris J R, Ho K M *et al. Metallurgical and Material Transactions A*[J], 2002, 33A: 851

8 Trojanová Zuzanka, Luká Pavel. *Engineering Procedia*[J], 2011, 10: 2318

9 Lichý P, Cagala M. *Archives of Foundry Engineering*[J], 2012, 12(2): 49

10 Song Jiangfeng, She Jia, Chen Daolun *et al. Journal of Magnesium and Alloys*[J], 2020, 8(1): 1

11 Mordike B L, Ebert T. *Material Science and Engineering A*[J], 2001, 302(1): 37

12 Wu R, Yan Y, Wang G *et al. International Materials Reviews*[J], 2015, 60(2): 65

13 Wu Ruizhi, Guo Xuyin, Li Dayong. *Journal of Alloys and Compounds*[J], 2014, 616: 408

14 Makhlouf H A S. *Intelligent Coatings for Corrosion Control*[M]. Amsterdam: Butterworth-Heinemann, 2015: 537

15 StJohn David, Nie Jianfeng. *Light Alloys*[M]. UK: Butterworth-Heinemann, 2017: 287

16 Monteiro W A, Buso S J, da Silva L V. *New Features of Magnesium Alloys*[M]. Rijeka: IntechOpen, 2012: 161

17 Koc Erkan, Turan Muhammet Emre. *Materials Research Express* [J], 2019, 8(6): 1

18 Ramalingam Vaira Vignesh, Ramasamy Padmanaban, Kovukkal Mohan Das *et al. Metals and Materials International*[J], 2019, 26(4): 409

19 Friedrich H, Schumann S. *Journal of Materials Processing Technology*[J], 2001, 117: 276

20 Schumann S. *Materials Science Forum*[J], 2005, 488-489: 1

21 Mordike B L, Ebert T. *Material Science and Engineering A*[J], 2001, 302: 37

22 Brooks E K, Ehrensberger M T. *Journal of Functional Biomaterials*[J], 2017, 8(3): 38

23 Zheng Tianxu, Hu Yaobo, Yang Shengwei. *Journal of Magnesium and Alloys*[J], 2017, 5(4): 404

24 Harrison Richard, Maradze Diana, Lyons Simon *et al. Progress in Natural Science Materials International*[J], 2014, 24(5): 539

25 Zhang Chunhong, Huang Xiaomei, Zhang Milin *et al. Materials Letters*[J], 2008, 62(14): 2177

26 Mousa H M, Hussein K H, Woo H M *et al. Ceramics International*[J], 2015, 41(9): 10 861

27 Jia Hongmin, Feng Xiaohui, Yang Yuansheng. *Journal of Magnesium and Alloys*[J], 2015, 3(3): 247

28 Zhou Xuehua, Huang Yuanwei, Wei Zhongling *et al. Corrosion Science*[J], 2006, 48(12): 4223

29 Chu P W, Marquis E A. *Corrosion Science*[J], 2015, 101: 94

30 Yamauchi N, Ueda N, Okamoto A *et al. Surface Coatings and Technology*[J], 2007, 201: 4913

31 Haferkamp H, Niemeyer M, Boehm R *et al. Material Science Forum*[J], 2000, 350-351: 31

32 Han B Q, Dunand D C. *Material Science and Engineering A*[J], 2000, 277: 297

33 Klaumünzer D, Hernandez J V, Yi S *et al. Magnesium Technology*[M]. Cham: Springer, 2019: 15

34 Sankaran K K, Mishra R S. *Metallurgy and Design of Alloys with Hierarchical Microstructures*[M]. Amsterdam: Elsevier, 2017: 345

35 Kulekci M K. *International Journal of Advanced Manufacturing Technology*[J], 2008, 39(9-10): 851

36 Knochel P A. *Nature Chemistry*[J], 2009, 1: 740

37 Hirsch J, Al-Samman T. *Acta Materialia*[J], 2013, 61(3): 818

38 Counts W A, Friák M, Raabe D *et al. Acta Materialia*[J], 2009, 57(1): 69

39 Pan Fusheng, Yang Mingbo, Chen Xianhua. *Journal of Materials Science and Technology*[J], 2016, 32(12): 1211

40 Su Juan, Guo Feng, Cai Huisheng *et al. Journal of Physics and Chemistry of Solids*[J], 2019, 131: 125

41 Jiang Bin, Liu Xuhe, Wu Ruizhi *et al. Journal of Shanghai Jiaotong University (Science)*[J], 2012, 17(3): 297

42 Cheng Weili, Wang Weiwei, Wang Hongxia *et al. Material Science and Engineering A*[J], 2015, 633: 63

43 Białobrzeski A, Saja K. *Archives of Foundry Engineering*[J], 2011, 11(3): 17

44 Wang H, Zhou B, Zhao Y *et al. Material Science and Engineering A*[J] ,2014, 589: 119

45 Cheng W, Tiang L, Bai Y *et al. Journal of Materials Research* [J], 2017, 32(12): 1

46 Park G H, Kim J T, Park J H *et al. Journal of Alloys and Compounds*[J], 2016, 680: 116

47 Alaneme K K, Okotete E A. *Journal of Magnesium and Alloys* [J], 2017, 5(4): 460

48 Zeng Ying, Jiang Bin, Huang Dehui *et al. Journal of Magnesium and Alloys*[J], 2013, 1(4): 1

49 Jiang Bin, Yang Qingshan, Zhang Mingxing *et al. Progress in Natural Science: Materials International*[J], 2011, 21(3): 236

50 Lamark T T, Hellmig R J, Estrin Y. *Material Science Forum*[J], 2006, 503-504: 889

51 Król Mariusz. *Solid State Phenomena*[J], 2018, 275: 41

52 Kral M V, Muddle B C, Nie J F. *Material Science and Engineering A*[J], 2007, 460-461: 227

53 Shin I, Carter E A. *Acta Materialia*[J], 2013, 64: 198

54 Rahulan N, Gopalan S, Kumaran S. *Materials Today Proceedings*[J], 2018, 5(9): 17 935

55 Li H B, Yao G C, Guo Z Q *et al. Acta Metallurgica Sinca*[J], 2006, 19(5): 355

56 Song G S, Staiger M, Kral M. *Material Science and Engineering A*[J], 2004, 371: 371

57 Chiu C H, Wang J H, Wu H Y. *Material Science Forum*[J], 2007, 546-549: 229

58 Lowe T C, Valiev R Z. *The Journal of Minerals, Metals & Materials Society*[J], 2004, 56(10): 64

59 Estrin Y, Vinogradov A. *Acta Materialia*[J], 2013, 61(3): 782

60 Cao Yang, Ni Song, Liao Xiaozhou *et al*. *Material Science and Engineering R*[J], 2018, 133: 1

61 Langdon T G. *Material Science and Engineering A*[J], 2007, 462(1-2): 3

62 Yang Y, Peng X, Ren F *et al. Journal of Material Science and Technology*[J], 2016, 32(12): 1289

63 Jiang B, Yang Q S, Gao L *et al. Materials Science Forum*[J], 2011, 686: 90

64 Liu T, Wu S D, Li S X *et al. Material Science and Engineering A*[J], 2007, 460-461: 499

65 Zhang S, Li M, Wang H *et al. Materials*[J], 2018, 11: 136

66 Gan W M, Wu K, Zheng M Y *et al. Material Science and Engineering A*[J], 2009, 516: 283

67 Rosochowski A, Olejnik L. *Severe Plastic Deformation for Grain Refinement and Enhancement of Properties*[M]. Cambridge: Woodhead Publishing Limited, 2012: 114

68 Wang Yang, Liao Yang, Wu Ruizhi *et al. Material Science and Engineering A*[J], 2020, 787: 139 494

69 Wang Yangbo, Liao Xiaozhou, Zhu Yuntian. *International Journal of Materials Research*[J], 2009, 100(12): 1632

70 Bay B, Hansen N, Hughes D A *et al. Acta Metallurgica et Materialia*[J], 1992, 40(2): 205

71 Liu Q, Jensen D J, Hansen N. *Acta Materialia*[J], 1998, 46(16): 5819

72 Kratochvíl Jan. *Materials Science Forum*[J], 2011, 667-669: 617

73 Figueiredo R B, Beyerlein I J, Zhilyaev A P *et al. Material Science and Engineering A*[J], 2010, 527(7-8): 1709

74 Sastry S M L, Mahapatra R N. *Material Science and Engineering A*[J], 2001, 329-331: 872

75 Minarik Peter, Cizek Jakub, Veseyl Jozef *et al. Materials Characterization*[J], 2017, 127: 258

76 Chiang C T, Lee S, Chu C L. *Transactions of Nonferrous Metals Society of China*[J], 2010, 20(8): 1374

77 Tang Yan, Le Qichi, Jia Weitao *et al. Material Science and Engineering A*[J], 2017, 704: 344

78 Lu L, Schwaiger R, Shan Z W *et al. Acta Materialia*[J], 2005, 53: 2169

79 Radhi H N, Aljassani A M H, Mohammed M T. *Materials Today Proceedings*[J], 2020, 26: 2302

80 Dobatkin S V, Valiev R Z, Krasil'nikov N A *et al. Metal Science and Heat Treatment*[J], 2000, 42(9-10): 366

81 Furukawa M, Horita Z, Nemeto M *et al. Journal of Materials Science*[J], 2001, 36: 2835

82 Iwahashi Yoshinori, Wang Jingtao, Horita Zenji *et al. Scripta Materialia*[J],1996, 35(2): 143

83 Ciemiorek Marta, Orlowska Marta, Lewandowska Malgorzata. *Advanced Engineering Materials*[J], 2020, 22(1): 1 900 666

84 Valiev R Z, Langdon T G. *Progress in Material Science*[J], 2006, 51: 881

85 Tyagi A K, Bunerjee S. *Materials Under Extreme Conditions: Recent Trends and Future Prospects*[M]. India: Elsevier, 2017: 717

86 Langdon T G, Furukawa M, Nemoto M *et al. Materials Science Forum*[J], 2001, 357-359: 489

87 Liu Y, Liu Manping, Chen Xuefei *et al. Scripta Materialia*[J], 2019, 159: 137

88 Huang Y, Prangnell P B. *Scripta Materialia*[J], 2007, 56: 333

89 Zhu Y T, Kolobov Y R, Grabovetskaya G P *et al. Journal of Materials Research*[J], 2003, 18(4): 1011

90 Avvari M, Narendranath S, Nayaka H S. *International Journal of Materials and Product Technology*[J], 2015, 51(2): 139

91 Lei Weiwei, Zhang Hui. *Materials Letters*[J], 2020, 271: 127 781

92 Li B, Joshi S, Azevedo K *et al. Material Science and Engineering A*[J], 2009, 517: 24

93 Semiatin S L, Segal V M, Goforth R E *et al. Metallurgical and Materials Transaction A*[J], 1999, 30A: 1425

94 Guo Fei, Liu Liu, Ma Yanlong *et al. Material Science and Engineering A*[J], 2020, 772: 138 792

95 Figueiredo R B, Cetlin P R, Langdon T G. *Acta Materialia*[J], 2007, 55: 4769

96 Málek P, Cieslar M, Islamgaliev R K. *Journal of Alloys and Compounds*[J], 2004, 378: 237

97 Kim H, Lee Y, Chung C. *Scripta Materialia*[J], 2005, 52: 473

98 Iwahashi Yoshinori, Horita Zenji, Nemoto Minoru *et al. Acta Materialia*[J], 1988, 46(9): 3317

99 Gopi K R, Nayaka H S, Sahu S. *Journal of Materials Engineering and Performance*[J], 2016, 25(9): 1

100 Zhao Zude, Chen Qiang, Hu Chuankai *et al*. *Materials Design* [J], 2009, 30(10): 4557

101 Ding R G, Chung C W, Chiu Y L. *Journal of Physics: Conference Series*[J], 2010, 241: 1

102 Kim W J, Jeong H G. *Material Science Forum*[J], 2003, 419-422: 201

103 Gopi K R, Shivananda Nayaka H, Sahu S. *Arabian Journal for Science and Engineering*[J], 2017, 42(11): 4635

104 Suh Joungsik, Victoria-Hernandez Jose, Letzig Dietmar *et al*. *Materials Science and Engineering A*[J], 2016, 669: 159

105 Tong L B, Chu J H, Sun W T *et al*. *Journal of Magnesium and Alloys*[J], 2020, 9(3): 1007

106 Ma Aibin, Jiang Jinghua. *Magnesium Alloys-Design, Processing and Properties*[M]. Rijeka: InTech, 2011: 187

107 Zhou Zhou, Song Dan, Liang Ningning *et al. Materials*[J], 2019, 12: 3255

108 Wu Haoran, Jiang Jinghua, Liu Huan *et al. Metals*[J], 2017, 7(12): 563

109 Kim J C, Nishida Y, Arima H *et al. Materials Letters*[J], 2003, 57: 1689

110 Liu Huan, Ju Jia, Bai Jing *et al. Metals*[J], 2017, 7: 398

111 Nishida Y, Sigematsu I, Arima H *et al. Journal of Material Science Letters*[J], 2002, 21: 465

112 Ma Aibin, Nishida Yoshinori, Suzuki Kazutaka *et al. Scripta Materialia*[J], 2005, 52(6): 433

113 Vishnu P, Raj M R, Krishna S E *et al. Materials Today Proceeding*[J], 2020, 21: 212

114 Watazu Akira, Shigematsu Ichinori, Hakamada Masataka *et al. Materials Science Forum*[J], 2010, 638-642: 1614

115 Huang He, Liu Huan, Wang Ce *et al. Journal of Magnesium and Alloys*[J], 2019, 7(4): 1

116 Xu Qiong, Ma Aibin, Li Yuhua *et al. Materials*[J], 2019, 12(21): 1

117 Xu Qiong, Ma Aibin, Li Yuhua *et al. Journal of Magnesium and Alloys*[J], 2020, 8(1): 192

118 Xu Bingqian, Sun Jiapeng, Yang Zhenquan *et al. Materials Science and Engineering A*[J], 2020, 780: 139 191

119 Ma Aibin, Jiang Jinghua, Saito Naobumi *et al. Materials Science and Engineering A*[J], 2009, 513-514: 122

120 Ma Ying, Liu Cheng, Li Mingzhe. *Acta Metallurgica Sinca (English Letters)*[J], 2020, 33: 233

121 Wang Ce, Ma Aibin, Sun Jiapeng *et al. Metals*[J], 2019, 9(7): 767

122 Mesbah Mohsen, Fadaeifard Firouz, Karimzadeh Atefeh *et al. Metals and Materials International*[J], 2016, 22(6): 1098

123 Faraji G, Mosavi M M, Kim H S. *Materials Transactions*[J], 2012, 53(1): 8

124 Javidikia M, Hashemi R. *Transactions of the Indian Institute of Metals*[J], 2017, 70(10): 2547

125 Djavanroodi F, Ebrahimi M. *Material Science and Engineering A*[J], 2010, 527(29-30): 7593

126 Raab G I. *Material Science and Engineering A*[J], 2005, 410-411: 230

127 Faraji G, Babaei A, Mosavi M M *et al. Materials Letters*[J], 2012, 77: 82

128 Faraji G, Mosavi M M, Kim H S. *Materials Letters*[J], 2011, 65(19-20): 3009

129 Faraji G, Mosavi M M, Abrinia K *et al. Applied Physics A*[J], 2012, 107(4): 819

130 Eftekhari M, Fata A, Faraji G *et al. Journal of Alloys and Compounds*[J], 2018, 742: 442

131 Fata A, Faraji G, Mashhadi M M *et al. Transactions of the Indian Institute of Metals*[J], 2017, 70: 1369

132 Fata A, Faraji G, Mashhadi M M *et al. Materials Science and Engineering A*[J], 2016, 674: 6

133 Mesbah M, Fatthai A, Bushroa A R *et al. Metals and Materials International*[J], 2021, 27: 277

134 Rosochowski Andrzej, Olejnik Lech. *Key Engineering Materials*[J], 2013, 554-557: 869

135 Olejnik L, Rosochowski A, Richert M W. *Material Science Forum*[J], 2008, 584-586: 108

136 Rosochowski Andrezj, Olejnik Lech. *Material Science Forum* [J], 2011, 674: 19

137 Gzyl Michal, Rosochowski Andrzej, Yakushina Evgenia *et al. Key Engineering Materials*[J], 2013, 554-557: 876

138 Qarni M J, Sivaswamy G, Rosochowski A *et al. Materials and Design*[J], 2017, 122: 385

139 Gzyl Michal, Rosochowski Andrzej, Boczkal Sonia *et al. Advanced Engineering Materials*[J], 2016, 18(2): 219

140 Gzyl Michal, Rosochowski Andrzej, Pesci Raphael *et al. Metallurgical and Materials Transactions A*[J], 2014, 45: 1609

141 Gzyl Michal, Rosochowski Andrzej, Boczkal Sonia *et al. Materials Science and Engineering A*[J], 2015, 638: 20

142 Gzyl Michal, Rosochowski Andrzej, Olejnik Lech *et al. Key Engineering Materials*[J], 2014, 611-612: 573

143 Kvackaj T, Kovacova A, Kocisko R *et al. Materials Characterization*[J], 2017, 134: 246

144 Chung Y H. *Material Science Forum*[J], 2010, 638-642: 1917

145 Chung Y H, Park J W, Lee K H. *Material Science Forum*[J], 2007, 539-543: 2872

146 Lee J C, Seok H K, Suh J Y. *Acta Materialia*[J], 2002, 50(16): 4005

147 Hassani F Z, Ketabchi M, Hassani M T. *Journal of Materials Science*[J], 2011, 46(24): 7689

148 Cheng Y Q, Chen Z H, Xia W J. *Materials Characterization*[J], 2007, 58(7): 617

149 Chen Z H, Cheng Y Q, Xia W J. *Materials and Manufacturing Processes*[J], 2007, 22(1): 51

150 Hassani F Z, Ketabchi M. *Material Science and Engineering A* [J], 2011, 528(21): 6426

151 Shi Laixin, Liu Lei, Hu Li *et al. Materials*[J], 2020, 13(15): 3346

152 Cheng Y Q, Chen Z H, Xia W J *et al. Journal of Materials Engineering and Performance*[J], 2008, 17: 15

153 Cheng Y Q, Chen Z H, Xia W J *Journal of Materials Science* [J], 2007, 42: 3552

154 Blum W, Dvořák J, Král P *et al. Journal of Materials Science and Technology*[J], 2016, 32(12): 1309

155 Kawasaki M, Horita Z, Langdon T G. *Material Science and Engineering A*[J], 2009, 524: 143

156 Huang Y, Prangnell P B. *Acta Materialia*[J], 2008, 56(7): 1619

157 Mishra A, Richard V, Gregori F *et al. Materials Science Forum* [J], 2006, 503-504: 25

158 Cabibbo M, Blum W, Evangelista E *et al. Metallurgical and Materials Transactions A*[J], 2008, 39A(1): 181

159 Hansen Niels. *Scripta Materialia*[J], 2004, 51: 801

160 Drozd Zdenek, Trojanová Zuzanka, Kúdela Stanislav. *Journal of Alloys and Compounds*[J], 2004, 378(1-2): 192

161 Tengen T B, Wejrzanowski T, Iwankiewicz R *et al. Solid State Phenomena*[J], 2008, 140: 185

162 Chang S Y, Lee S W, Kang K M *et al. Materials Transactions* [J], 2004, 45(2): 488

163 Trojanova Zuzanka, Drozd Zdenek, Lukac Pavel *et al. Material Science Forum*[J], 2003, 419-422: 817

164 Song Dan, Wang Guowei, Zhou Zhikai *et al. Material Science and Engineering A*[J], 2020, 773: 138 880

165 Kitahara Hiromoto, Maruno Fumiaki, Tsushida Masayuki *et al. Materials Science and Engineering A*[J], 2014, 590: 274

166 Figueiredo R B, Langdon T G. *Materials Science and Engineering A*[J], 2009, 501: 105

167 Poggiali F S J, Figueiredo R B, Aguilar M T P *et al. Materials Research*[J], 2012, 15(2): 312

168 Li Jizhong, Xu Wei, Wu Xiaolin *et al. Materials Science and Engineering A*[J], 2011, 528(18): 5993

169 Klu E E, Song D, Li C *et al. Metals*[J], 2019, 9: 1008

170 Chang L L, Wang Y N, Zhao X *et al. Materials Science and Engineering A*[J], 2008, 496(1-2): 512

171 Hsiang S H, Lin Y W. *Journal of Materials Processing Technology*[J], 2007, 192-193: 292

172 Yang H J, Shao X H, Li S X *et al. Materials Science Forum*[J], 2011, 667-669: 839

173 Minárik Peter, Král Robert, Pesicka Josef *et al. Journal of Materials Research and Technology*[J], 2015, 4(1): 75

174 Kapoor R, Kumar N, Mishra R S *et al. Materials Science and Engineering A*[J], 2010, 527(20): 5246

175 Zou Yun, Zhang Lehao, Wang Hongtao *et al. Journal of Alloys and Compounds*[J], 2016, 669: 72

176 Janecek M, Yi S, Kral R *et al. Journal of Materials Science*[J], 2010, 45: 4665

177 Liu T, Zhang W, Wu S D *et al. Materials Science and Engineering A*[J], 2003, 360: 345

178 Nemcko M J, Wilkinson D S. *International Journal of Fracture* [J], 2016, 200(1-2): 31

179 Valiev R Z, Alexandrov I V. *Journal of Materials Research*[J], 2002, 17(1): 5

180 Liu F, Liu Y, Wang J T. *Materials Science Forum*[J], 2016, 850: 419

181 Chang T C, Wang J Y, Chu C L *et al. Materials Letters*[J], 2006, 60(27): 3272

182 Langdon T G. *Solid State Phenomena*[J], 2020, 306: 1

183 Figueiredo R B, Langdon T G. *Advanced Engineering Materials* [J], 2008, 10(1-2): 37

184 Zeng Ying, Jiang Bin, Zhang Mingxing *et al. Intermetallics*[J], 2014, 45: 18

185 Prasad Y V R K, Ravichandran N. *Bulletin of Materials Science* [J], 1991, 14(5): 1241

186 Suresh M, Sharma A, More A M *et al. Journal of Alloys and Compounds*[J], 2019, 785: 972

187 Kang S H, Lee Y S, Lee J H *et al. Journal of Materials Processing Technology*[J], 2008, 201(1-3): 436

188 Almajid A A, El-Danaf A E, Soliman M S. *Journal of Materials Science*[J], 2009, 44: 5654

189 Oh-Ishi Keiichiro, Horita Zenji, Nemoto Minoru *et al. Metallurgical and Materials Transactions A*[J], 1988, 29A(7): 2011

190 Mousavi E S, Khaleghifar H M, Meratian M *et al. Materialia* [J], 2018, 4: 310

191 Uesugi Tokuteru, Kohyama Masanori, Kohzu Masahide *et al. Materials Science Forum*[J], 2000, 350-351: 49

192 Wang Jingfeng, Xu Dandan, Lu Ruopeng *et al. Transactions of Nonferrous Metals Society of China*[J], 2014, 24(2): 334

193 Yan Changjian, Xin Yunchang, Wang Ce *et al. Journal of Materials Science Technology*[J], 2020, 52: 89

194 Agnew S R, Yoo M H, Tomé C N. *Acta Materialia*[J], 2001, 49(20): 4277

195 Feng L P, Chen B, Liu P Y *et al. Materials Science Forum*[J], 2005, 475-479: 481

196 Agnew S R, Mehrotra P, Lillo T M *et al. Acta Materialia*[J], 2005, 53(11): 3135

197 Shah S S A, Sang H, Sun L B *et al. Russian Journal of Non-Ferrous Metals*[J], 2020, 61(3): 280

198 Agnew S R, Horton J A, Lillo T M *et al. Scripta Materialia*[J], 2004, 50(3): 377

199 Zou Yun, Zhang Lehao, Li Yang *et al. Journal of Alloys and Compounds*[J], 2017, 735: 2625

200 Lentz M, Klaus M, Beyerlein I J *et al. Acta Materialia*[J], 2015, 86: 254

201 Liu T, Wang Y D, Wu S D *et al. Scripta Materialia*[J], 2004, 51: 1057

202 Karami M, Mahmudi R. *Materials Science and Engineering A* [J], 2014, 607: 512

203 Wang Tianzi, Zhu Tianlong, Sun Jianfeng *et al. Journal of Magnesium Alloys*[J], 2015, 3(4): 345

204 Zeng Z, Stanford N, Davies C H J *et al. International Materials Revisions*[J], 2019, 64(1): 27

205 Wang Guowei, Song Dan, Li Chen *et al. Metals*[J], 2019, 9: 920

206 Crawford P, Barrosa R, Mendez J *et al. Journal of Materials Processing Technology*[J], 1996, 56: 108

207 Wu H Y, Yan J C, Tsai H H *et al. Materials Science and Engineering A*[J], 2010, 527(27-28): 7197

208 Cui Chongliang, Zhu Tianlong, Zhang Tianlong *et al. International Journal of Materials Research*[J], 2014, 105(11):

1111

209 Wang Jingfeng, Xu Dandan, Lu Ruopeng *et al. Transactions of Nonferrous Metals Society of China*[J], 2014, 24(2): 334

210 Yoo M H, Morris J R, Ho K M. *Metallurgical and Materials Transactions A*[J], 2002, 33A(3): 813

211 Figueiredo R B, Langdon T G. *Journal of Materials Research and Technology*[J], 2017, 6(2): 129

212 Zhao Jun, Jiang Bin, Tang Aitao *et al. Metals and Materials International*[J], 2019, 27: 1403

213 Mineta Takahiro, Hasegawa Kaoru, Sato Hiroyuki. *Materials Science and Engineering A*[J], 2020, 773: 138 867

214 Cain W J, Labukas J P. *Materials Degradation*[J], 2020, 4: 17

215 Dutkiewicz J, Rusz W, Maziarz W *et al. Acta Physica Polonica A*[J], 2017, 113(5): 1303

216 Karami M, Mahmudi R. *Metallurgical and Materials Transactions A*[J], 2013, 44: 3934

等通道转角挤压对Mg-Li合金力学性能的影响概述

Edwin Eyram Klu[1]，江静华[1,2]，Bassiouny Saleh[1,3]，马爱斌[1,2]，Salifu Nasiru[1]，宋　丹[1,2]

(1. 河海大学 力学与材料学院，江苏 南京 210098)

(2. 宿迁市河海大学研究院，江苏 宿迁 223800)

(3. 亚历山大大学 生产工程系，埃及 亚历山大 21544)

摘　要：等通道转角挤压（ECAP）是一种高效率的大塑性变形（SPD）技术，用于生产具有优异性能的超细晶粒（UFG）材料。本文总结了经ECAP加工的各种Mg-Li合金的力学性能、加工参数的影响及其相关机理，为未来提高镁锂合金力学性能提供研究方向与支持。

关键词：镁锂合金；等通道转角挤压；大塑性变形；力学性能；微观组织

作者简介：Edwin Eyram Klu，男，1982年生，博士生，河海大学力学与材料学院，江苏 南京 210098，E-mail：kluedwin@outlook.com